JOURNAL OF COMPUTATIONAL PHYSICS 93, 388–410 (1991)

Solution of the Implicitly Discretised Reacting Flow Equations by Operator-Splitting

R. I. ISSA

Department of Mineral Resources Engineering, Imperial College of Science, Technology and Medicine, London, England

AND

B. AHMADI-BEFRUI,* K. R. BESHAY,† AND A. D. GOSMAN

Department of Mechanical Engineering, Imperial College of Science, Technology and Medicine, London, England

Received April 24, 1987; revised November 14, 1989

The PISO method, which is a non-iterative method for the solution of the time-dependent, implicitly discretised fluid flow equations by operator-splitting, is extended here to handle reacting flows. The additional species conservation equations, together with the energy equation, are incorporated into the predictor–corrector sequence of steps. Both turbulent-mixing and chemical-kinetics controlled combustion models are catered to. The method is tested in one- and two-dimensional cases and a comparison with a comparable iterative scheme is made. The results show that such reacting flows can be handled by the new scheme with efficiency, while temporal accuracy is maintained.

INTRODUCTION

In [1], a non-iterative technique, called PISO, for the solution of the implicitly discretised time-dependent flow equations was described. The method was formulated for both laminar and turbulent inert flows, both compressible and incompressible. The non-iterative solution is accomplished at each time-step through a sequential predictor–corrector process within which the different dependent variables are updated individually. The term "operator-splitting" is invoked to refer to the separate operations effected to each of the variable fields, rather than to what is normally understood to be the time-splitting of terms. The avoidance of iteration at each time-step reduces the computing effort substantially, while the sequential nature of the solution obviates the need for block solution and its complexity.

* Present address: Faculty of Engineering, Cairo University, Egypt.
† Present address: AVL, Graz, Austria.

0021-9991/91 $3.00

The performance of the PISO method was evaluated in [2], where it was applied to compressible and incompressible flows. A comparison with similar computations using iteration verified the considerable advantages of PISO in speed.

As was pointed out in [1], the predictor–corrector strategy need not be confined to the handling of the linear coupling between the equations in pressure and velocity. Extension of the method was indeed made to handle the strong coupling through the source terms in the $k-\varepsilon$ turbulence model equations. Here, a method, based on the PISO approach, to compute reacting flows is presented. Because of the strong coupling arising from large density variations, the scheme must now cope with non-linear linkages acting through the convective contributions in the equations. This is in addition to the coupling through the source terms due to the reaction kinetics.

The basic PISO method, in the form presented in [1], has in fact already been applied to steady-state reacting flows in, for example, [3, 4]. However, in these implementations, the splitting was effected only to the momentum and continuity equations, while the handling of the conservation equations for species and temperature (pertaining to the combusion process) was merely appended at the end of the splitting sequence. No attempt was made to absorb the coupling between those two sets of equations within the splitting procedure.

Although the above applications have demonstrated the utility and reliability of PISO, they do not take advantage of the strength of the method by incorporating all strongly coupled equations within the splitting process. More importantly, PISO was primarily devised to handle unsteady flow efficiently by avoiding iteration, which is made possible by this very splitting practice. Clearly, such a capability cannot be maintained when extension to reacting flows is made without the incorporation of the equations governing combustion within the splitting process. It is this issue which is dealt with herein.

It should be emphasized here, that the present method is mainly intended to cater to the strong coupling between the flow field and the combustion process, rather than to deal exclusively with the "stiffness" of the combustion equations themselves which is inherent in the modelling of chemical reactions. Such stiffness can itself be handled by operator-splitting, as examination of the literature would reveal (see, for example, [5, 6]). In the latter context operator splitting is introduced into the species equations alone to cope with two disparate time-scales, that of the combustion process and that of transport, regardless of the two-way coupling between the flow and combustion process. Such splitting can indeed be incorporated within the method presented herein. However, for the purpose of this study, no such measures (save for the linearisation of one term to be outlined later) were found necessary. This was partly assisted by the fact that only single-step reactions were considered; it can also be argued that the implicit treatment of the reaction terms, facilitated by the present method, must have been another main factor. It should be stressed that the capability of the method to handle multi-step reactions remains to be verified.

Since the present work is concerned with the method of solution rather than with the modelling of reaction processes, little will be said about the combustion models

themselves. The handling of two such models is treated herein; the first is the conventional Arrhenius type for chemical-kinetics controlled combustion, and the second is for turbulent-mixing controlled reaction due to [7]. The method will be explained with reference to a simple example in which two species (fuel and oxidant) react to give one product. The following sections will first present the governing equations to be solved, the operator-splitting procedure will then be detailed, and finally results of the computations will be compared with calculations performed using a comparable iterative method.

Governing Equations and Discretisation

The Transport Equations

The governing ensemble-averaged transport equations in Cartesian tensor notation for continuity, momentum, energy, and species (fuel) in reacting flow are

$$\frac{\partial \rho}{\partial t} + \frac{\partial}{\partial x_j}(\rho u_j) = 0 \tag{1}$$

$$\frac{\partial}{\partial t}(\rho u_i) + \frac{\partial}{\partial x_j}(\rho u_i u_j) = -\frac{\partial p}{\partial x_i} + \frac{\partial}{\partial x_j}\left(\mu \frac{\partial u_i}{\partial x_j}\right) \tag{2}$$

$$\frac{\partial}{\partial t}(\rho e) + \frac{\partial}{\partial x_j}(\rho u_j e) = -p\frac{\partial u_j}{\partial x_j} + \frac{\partial}{\partial x_j}\left(\frac{\mu}{\sigma_E}\frac{\partial e}{\partial x_j}\right) \tag{3}$$

and

$$\frac{\partial}{\partial t}(\rho m_f) + \frac{\partial}{\partial x_j}(\rho u_j m_f) = \frac{\partial}{\partial x_j}\left(\frac{\mu}{\sigma_F}\frac{\partial m_f}{\partial x_j}\right) + S_F, \tag{4}$$

where all dependent variables are taken to be the ensemble-averaged mean when the flow is turbulent, and μ is an effective viscosity, while σ_E and σ_F are effective Prandtl numbers. Presently, these diffusion coefficients are assumed to be given. In turbulent flow, their values might be determined from a turbulence model such as the $k-\varepsilon$ one; otherwise laminar values prevail. When a turbulence model is used, the associated equations should be handled within the splitting procedure. As this is outlined in [1], reference to it will be omitted here. The energy, e, is related to the temperature, T, and the fuel mass fraction (also referred to as concentration), m_f, by

$$e = C_v T + m_f H_c, \tag{5}$$

where C_v is the constant volume specific heat, and H_c is the heat of combustion of the fuel. Term S_F in Eq. (4) stands for the rate of consumption of fuel.

The pressure, p, and the density, ρ are related by the equation of state which may be written in the form

$$\rho = p\psi(p, T), \tag{6}$$

where, for a perfect gas, ψ becomes $1/RT$.

The main heat-releasing combustion reaction is presumed to be of the global single-step irreversible form

$$1 \text{ kg fuel} + s \text{ kg oxidant} \rightarrow (1+s) \text{ kg products}, \tag{7}$$

where s is the stoichiometric combination ratio.

The fuel combustion rate, S_F, for a chemical-kinetics controlled combustion process is represented by the Arrhenius type expression

$$S_F = -A\rho^2 m_f m_o \exp\left(-\frac{E}{RT}\right), \tag{8}$$

where A and E are empirical coefficients, m_o is the concentration (mass fraction) of oxidant, and R is the universal gas constant. For turbulent-mixing controlled combustion, the expression proposed in [7] is used. It is

$$S_F = -A' \frac{\rho}{\tau} \min\left\{m_f, \frac{m_o}{s}, \frac{Bm_p}{1+s}\right\}, \tag{9}$$

where A' and B are empirical coefficients, and τ is the turbulent-mixing time scale. The mass fractions of oxidant and product, denoted by m_o and m_p, respectively, along with the inert concentration, m_i, are obtained through Eq. (7) and the overall species conservation as

$$\begin{aligned} m_f - \frac{m_o}{s} &= m_{f,I} - \frac{m_{o,I}}{s} \\ m_f + \frac{m_p}{1+s} &= m_{f,I} + \frac{m_{p,I}}{1+s} \end{aligned} \tag{10}$$

and

$$\sum_j m_j = 1, \qquad j = f, o, p, i,$$

where the subscript I denotes an initial value.

Discretisation

As is the case with the basic PISO method in [1], the splitting procedure can be effected to any set of equations discretised by conventional difference schemes. For the sake of generality, the discretised equations are therefore presented here in the

operator form employed in [1], which caters to the various spatial discretisation schemes. For temporal discretisation, the Euler implicit scheme is again selected for ease of presentation.

The governing equations (1) to (4) may be expressed, respectively, as:

$$\frac{1}{\delta t}(\rho^{n+1}-\rho^n)+\Delta_i(\rho u_i)^{n+1}=0 \tag{11}$$

$$\frac{1}{\delta t}\{(\rho u)^{n+1}-(\rho u)^n\}-A_0 u_i^{n+1}=H(u_i^{n+1})-\Delta_i p^{n+1} \tag{12}$$

$$\frac{1}{\delta t}\{(\rho e)^{n+1}-(\rho e)^n\}-B_0 e^{n+1}=J(e^{n+1})-p^{n+1}\Delta_i u_i^{n+1} \tag{13}$$

$$\frac{1}{\delta t}\{(\rho m_f)^{n+1}-(\rho m_f)^n\}-(C_0+S_0)m_f^{n+1}=G(m_f^{n+1})+S^{n+1}. \tag{14}$$

In Eqs. (11) to (14), similar notation and practices as those introduced in [1] are followed. Thus, the operators H, J, and G contain the convective and diffusive contributions and are defined as

$$H=\sum_k A_k u_{i,k} \tag{15}$$

$$J=\sum B_k e_k \tag{16}$$

and

$$G=\sum C_k m_{f,k}, \tag{17}$$

where index k is a grid node identifier and the summation is over all the nodes surrounding the central node that are involved in the formulation of the finite-difference representation of spatial fluxes. The quantities A, B, and C are finite-difference coefficients; subscript 0 denotes the central coefficient. These central elements are taken to the left-hand side of the equations to enable their implicit treatment in the manner introduced in [1].

The terms S and S_0 in the equation for species contain the rate of consumption of fuel, the expressions for which depend on the combustion model. Thus, for the turbulent-mixing controlled rate proposed in [7],

$$S=-A'\frac{\rho}{\tau}\min\left\{m_f,\frac{m_0}{s},\frac{Bm_p}{1+s}\right\} \tag{18a}$$

and

$$S_0=0 \tag{19a}$$

and, for an Arrhenius reaction rate,

$$S = -A\rho^2 s m_f (m_f - m) \exp\left(-\frac{E}{RT}\right) \tag{18b}$$

and

$$S_0 = -A\rho^2 s (2m_f - m) \exp\left(-\frac{E}{RT}\right), \tag{19b}$$

where

$$m = m_{f,I} - \frac{m_{0,I}}{s}.$$

In arriving at expressions (18b) and (19b), the reaction rate term, S_F, has been linearised in m_f using Taylor series expansion. This enhances the stability of the procedure as it strengthens the diagonal dominance in the set of discretised equations. This was the only measure found necessary to stabilise the calculations presented herein. This, it may be argued, is due to the simple single-step reaction considered here. Other linearisations (or operator-splittings in the sense used by [6]) of the source terms in cases of multi-step reactions may be necessary, in which case the resulting expressions could still be incorporated in the overall PISO splitting.

As in the case in [1], the pressure is computed from its own equation which is derived from a combination of the continuity equation (11) and the momentum equations (12). The derivation of such an equation will be dealt with when the solution algorithm is presented.

The above equations are general and do not relate to a particular spatial discretisation scheme. It is these equations which will be used in the presentation of the splitting algorithm. For the purpose of the example calculations presented later, however, one such scheme had to be selected. This is the same as that described in [2], and hence requires no further elucidation here. It suffices to say that the scheme employs a staggered grid, is of the finite-volume type, and is based on a hybrid of upwind/central difference formulae.

Splitting Procedure

In [1], the operator-splitting methodology was introduced to the equations of inert flow, in which the variations in density are solely due to compressibility. Attention was focused there on the linear pressure–velocity coupling and, although it was pointed out that non-linear coupling through coefficients can be handled by the same splitting procedure, this was ignored because it was deemed unnecessary for the applications in hand.

In reacting flows, very large density gradients arise, leading to strong non-linear coupling of the equations; this can no longer be ignored in the formulation of the solution algorithm. As will be seen shortly, the incorporation of the species and energy equations demand significant restructuring of the predictor and corrector steps in the algorithm. This restructuring embodies the main departures from the original splitting. These are:

(i) The energy as well as the species equations are now solved in implicit form together with momentum in the same predictor step. This is to account for the rapid variations in temperature and concentration over the time-step brought about by combustion and which have profound influence on subsequent corrector steps.

(ii) The coefficients in the corrector steps are now updated to reflect the large variations in density. The updating is carried out only after the continuity-based pressure equation is solved. This ensures that conservation is maintained, which is crucial especially in the calculation for species.

(iii) Energy and species corrector steps now follow each momentum corrector. This leads to an increase in the accuracy of the overall scheme (this can be shown following the analysis in [1]; hence it is not presented here).

Another change that is made is the solution for pressure itself rather than for pressure increments as in [1]. This is merely an organisational matter which does not affect the outcome of the calculations. The details of the splitting are presented in what follows.

Let superscripts *, **, and *** denote intermediate field values obtained during the splitting procedure. The steps in this procedure are as follows:

(a) *Predictor step.* The velocity, density, viscosity, and pressure field prevailing at time t^n are used to calculate the coefficients A, B, and C in Eq. (15) to (17). The governing equations are solved in the following sequence:

(i) Energy. Based on Eq. (13), this is:

$$\left(\frac{\rho^n}{\delta t} - B_0^n\right) e^* = J^n(e^*) + \frac{\rho^n}{\delta t} e^n - p^n \Delta_i u_i^n. \tag{20}$$

(ii) Species. From Eq. (14), this is:

$$\left(\frac{\rho^n}{\delta t} - C_0^n - S_0^n\right) m_f^* = G^n(m_f^*) + \frac{\rho^n}{\delta t} m_f^n + S^n. \tag{21}$$

(iii) Momentum. Equation (12) is taken as:

$$\left(\frac{\rho^n}{\delta t} - A_0^n\right) u_i^* = H^n(u_i^*) + \frac{\rho^n}{\delta t} u_i^n - \Delta_i p^n. \tag{22}$$

Equations (20), (21), and (22) can be solved by one of the standard techniques to yield the e^*, m_f^*, and u_i^* fields, the last of which, it should be noted, will not in

general satisfy the continuity equation (11). The temperature, T^*, is now calculated from Eq. (5). Note that the order of solution of these equations is of no consequence, as all coefficients are based on old time level values.

(b) *First corrector step.* (i) Momentum corrector. A new velocity field, u_i^{**}, together with corresponding pressure and density fields, p^* and ρ^*, are sought to satisfy the continuity equation:

$$\frac{1}{\delta t}(\rho^* - \rho^n) + \Delta_i(\rho^* u_i^{**}) = 0. \tag{23}$$

The momentum equation (12) is now written in an explicit corrector form as

$$\left(\frac{1}{\delta t} - \frac{A_0^n}{\rho^n}\right)\rho^* u_i^{**} = H^n(u_i^*) + \frac{\rho^n}{\delta t}u_i^n - \Delta_i p^*, \tag{24}$$

where all the coefficients A are still evaluated at the old time level (note that the velocities u_i^* and the density ρ^n do not satisfy continuity). Equations (23) and (24) are now used to derive the pressure equation in the fashion presented in [1]. Thus, taking the divergence of Eq. (24) and substituting into Eq. (23) gives

$$\left[\Delta_i\left\{\left(\frac{1}{\delta t} - \frac{A_0^n}{\rho^n}\right)^{-1}\Delta_i\right\} - \frac{\psi^*}{\delta t}\right]p^* = \Delta_i\left[\left(\frac{1}{\delta t} - \frac{A_0^n}{\rho^n}\right)^{-1}\left\{H^n(u_i^*) + \frac{\rho^n u_i^n}{\delta t}\right\}\right] - \frac{\rho^n}{\delta t}, \tag{25}$$

where, in arriving at Eq. (25), ρ^* has been replaced by:

$$\rho^* = p^*\psi^*. \tag{26}$$

Equation (25) can be solved for p^*; the new densities and velocities, ρ^* and u_i^{**}, are now computed from Eqs. (26) and (24), respectively. These new fields, it should be recalled, satisfy the continuity equation (23).

(ii) Energy corrector. The u_i^{**} and ρ^* which now satisfy continuity are used to update the B coefficient in equation (17). The energy corrector equation is thus taken as

$$\left(\frac{\rho^*}{\delta t} - B_0^*\right)e^{**} = J^*(e^*) + \frac{\rho^n}{\delta t}e^n - p^*\Delta_i u_i^{**} \tag{27}$$

which yields the e^{**} field.

(iii) Species corrector. Here, also, u_i^{**} and ρ^* are used to update the C coefficient in Eq. (16). The species corrector equation is

$$\left(\frac{\rho^*}{\delta t} - C_0^* - S_0^*\right)m_f^{**} = G^*(m_f^*) + \frac{\rho^n}{\delta t}m_f^n + S^* \tag{28}$$

which yields the m_f^{**} field. The temperature is then updated from Eq. (5) as

$$T^{**} = \frac{e^{**} - m_f^{**} H_c}{C_v}, \tag{29}$$

whence

$$\psi^{**} = \frac{1}{RT^{**}}. \tag{30}$$

(c) *Second corrector step.* (i) Momentum corrector. For this step, the momentum equation is

$$\left(\frac{1}{\delta t} - \frac{A_0^*}{\rho^*}\right) \rho^{**} u_i^{***} = H^*(u_i^{**}) + \frac{\rho^n}{\delta t} u_i^n - \Delta_i p^{**}, \tag{31}$$

where it should be noted that all A coefficients in Eq. (15) and (31) are based on ρ^* and u_i^{**}. By combining Eq. (31) with the continuity relation

$$\frac{1}{\delta t}(\rho^{**} - \rho^n) + \Delta_i(\rho^{**} u_i^{***}) = 0, \tag{32}$$

the following pressure equation is obtained:

$$\left[\Delta_i \left\{\left(\frac{1}{\delta t} - \frac{A_0^*}{\rho^*}\right)^{-1} \Delta_i\right\} - \frac{\psi^{**}}{\delta t}\right] p^{**} = \Delta_i \left[\left(\frac{1}{\delta t} - \frac{A_0^*}{\rho^*}\right)^{-1} \left\{H^*(u_i^{**}) + \frac{\rho^n u_i^n}{\delta t}\right\}\right] - \frac{\rho^n}{\delta t}. \tag{33}$$

In arriving at the last equation, the followinig equation of state has been invoked:

$$\rho^{**} = p^{**} \psi^{**}. \tag{34}$$

Solution of Eq. (33) yields p^{**} which is used to obtain ρ^{**}, via Eq. (34), and velocity u_i^{***} from Eq. (31).

(ii) Energy corrector. The coefficients B in the energy equation are updated using the most recent values of density and velocity to give the second energy corrector equation,

$$\left(\frac{\rho^{**}}{\delta t} - B_0^{**}\right) e^{***} = J^{**}(e^{**}) + \frac{\rho^n}{\delta t} e^n - p^{**} \Delta_i u_i^{***}, \tag{35}$$

which yields e^{***}.

(iii) Species corrector. Similarly, the second-corrector species equation is

$$\left(\frac{\rho^{**}}{\delta t} - C_0^{**} - S_0^{**}\right) m_f^{***} = G^{**}(m_f^{**}) + \frac{\rho^n}{\delta t} m_f^n + S^{**}, \tag{36}$$

which gives the m_f^{***} field. The temperature is then obtained from

$$T^{***} = \frac{e^{***} - m_f^{***} H_c}{C_v}. \tag{37}$$

The density ρ^{**}, velocity u_i^{***}, fuel concentration m_f^{***}, and temperature T^{***} are taken to represent the field values at the next time level, $n+1$; this completes the sequence in the solution of the equations over the time-step. It should be noted that, for non-reacting flows, the method reduces to the original PISO with coefficients being updated at each corrector step.

RESULTS

Preamble

The present methodology is applied to both one- and two-dimensional unsteady flame propagation in confined chambers. The purpose of the calculation is to:

(i) demonstrate that the method is capable of handling two different, single-step reaction models, including that of the Arrhenius type;

(ii) show, at least for the present choice of discretisation scheme, that the temporal errors introduced by the splitting procedure vanish with δt and do so at least as fast as the temporal discretisation error;

(iii) evaluate the saving in computing effort achieved by avoidance of iteration; and

(iv) demonstrate the ability of the method to handle large time steps when high temporal accuracy is not demanded.

To accomplish objectives (ii) and (iii) above, comparisons are made against computations with an existing iterative method employing the same spatial and temporal difference schemes. Such a method yields (by virtue of iteration) the exact solution (to within the iteration tolerance imposed of around 10^{-2} on residuals) to the discretised equations over each time-step. Hence, the errors in the fields thus calculated will be solely due to the spatial and temporal discretisation schemes. By refinement of δt, the value at which the chosen temporal difference scheme gives a time-accurate solution can therefore be found. Comparison with such solution at the same value of δt will reveal the temporal splitting errors contained in PISO.

latter, the species and energy equations are solved after momentum and pressure within each iteration. The reason for the choice is that the method is one of the most widely used and established. Improvements on SIMPLE have been developed in the form of the SIMPLER [9] and SIMPLEC [10] methods. These are reported to be more stable than SIMPLE and can be significantly faster when the

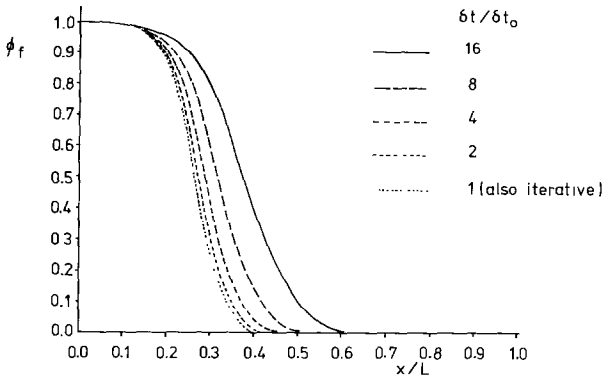

FIG. 1. Reactedness distribution for turbulent-mixing controlled reaction.

relaxation factors are optimised. The comparisons presented herein, therefore, have to be viewed with these improvements in mind. Nevertheless, the reported increase in speed with these methods is still not sufficient to offset the cost of iterating at each time-step, a process which the non-iterative PISO dispenses with.

One-Dimensional Compressible Reacting Flow

The one-dimensional compressible case chosen is that of a reacting flow with constant effective viscosity (values typical of a turbulent flow) in a long adiabatic duct with closed ends. The effects of wall shear are accounted for approximately. A uniform mesh of 200 cells was mainly used. In the absence of an ignition model, burning is triggered by artificially depleting the fuel in a small region (encompassing one computational cell) adjacent to one end of the duct, at a rate which consumes $\frac{1}{2}\%$ of the total charge over a period of τ, where τ is the mixing time scale, to be defined shortly; thereafter, combustion is allowed to proceed at its own rate.

Calculations were first performed for turbulent-mixing controlled combustion using the model in [7], with constants: $A = 4.0$ and $B = 0.5$. The turbulent mixing time scale, τ (0.01 s), and the viscosity levels are taken from other combustion simulations. The iterative scheme is used to find the maximum allowable value of the computational time-step (say, δt_0), for which the temporal truncation error is acceptably small.[1] Under-relaxation was necessary to stabilise the computations, values of 0.5 being used for the velocity, 0.7 for the energy and fuel concentration, and 1.0 for the pressure. Similar calculations were then performed using the present methodology using time-steps that are multiples of δt_0. Figures 1, 2, and 3 show the

[1] Only the final time-accurate solutions resulting from these exercises are presented for clarity.

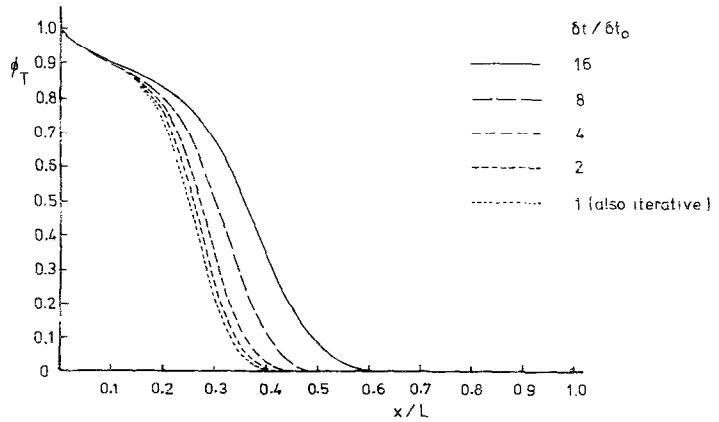

FIG. 2. Temperature distribution for turbulent-mixing controlled reaction.

predictions along the duct at time $t = 3\tau$. Figure 1 shows the distribution of the reactedness, defined as

$$\phi_f = \frac{m_f - m_f^u}{m_f^b - m_f^u},$$

where the superscripts u and b stand for unburnt and fully burnt values, respectively. Figure 2 shows the distribution of the normalised temperature, defined as

$$\phi_T = \frac{T - T^u}{T^b - T^u}$$

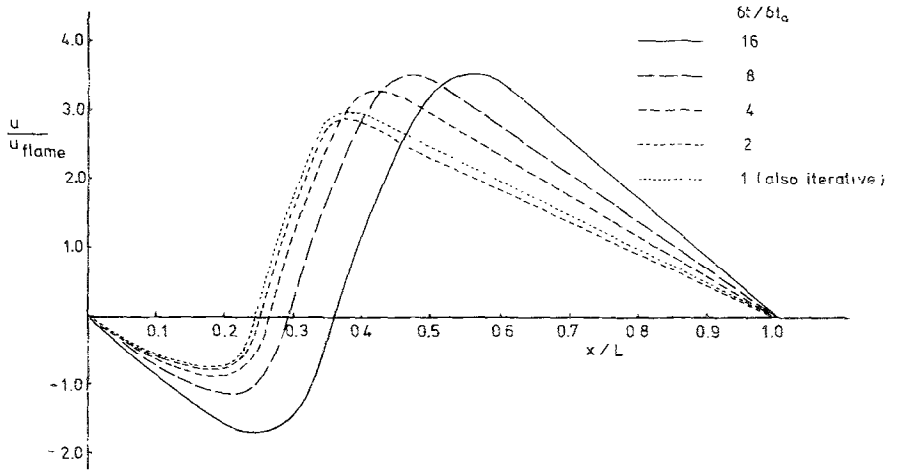

FIG. 3. Velocity distribution for turbulent-mixing controlled reaction.

and Fig. 3 displays the corresponding gas velocity normalised by the empirically determined turbulent flame speed ($\equiv 2\sqrt{C_\mu}\, ABk_0/\sigma_t$, where C_μ and σ_t are turbulence related constants, and k_0 is the initial turbulent kinetic energy). The reason for temperature rise behind the flame front in Fig. 2 is due to the pressure work term ($p(\partial u_j/\partial x_j)$) that appears in the energy equation (3); this is significant due to the steep velocity gradient and the low value of density behind the flame. The different curves in each case are those obtained with the present method for different values of $\delta t/\delta t_0$, as well as that for the time-accurate solution obtained with the iterative method. The latter curve is indistinguishable from that pertaining to $\delta t/\delta t_0 = 1$, verifying that the temporal splitting errors vanish before the errors introduced by the temporal difference scheme used.

Next, calculations were performed for a chemical-kinetics controlled reaction (Arrhenius) to test the performance of the present method for this difficult situation (where the reaction reate increases exponentially with temperature). The reaction rate constants are those for a pure hydrocarbon reaction and are taken as $A = 1.5 \times 10^8$ m^3/kg/s and $E = 1.0 \times 10^8$ J/kg mole. For this situation, the iterative scheme proved troublesome to converge and attempts to obtain a solution were abandoned because of the excessive computing time requirement. Figure 4 displays the results from PISO, where the effect of the computational time-step (normalised by the same value of τ as in the previous case, in the absence of a suitable time scale) on the calculated reactedness (φ_f) at $t = 3\tau$. The temporal truncation error becomes acceptably small at about $\delta t = 0.003\tau$. However, it could not be ascertained whether this is dictated by the temporal errors in the splitting or in discretisation, since no solutions could be obtained with the iterative method. Judging by the performance of PISO in the previous as well as the following cases, it is con-

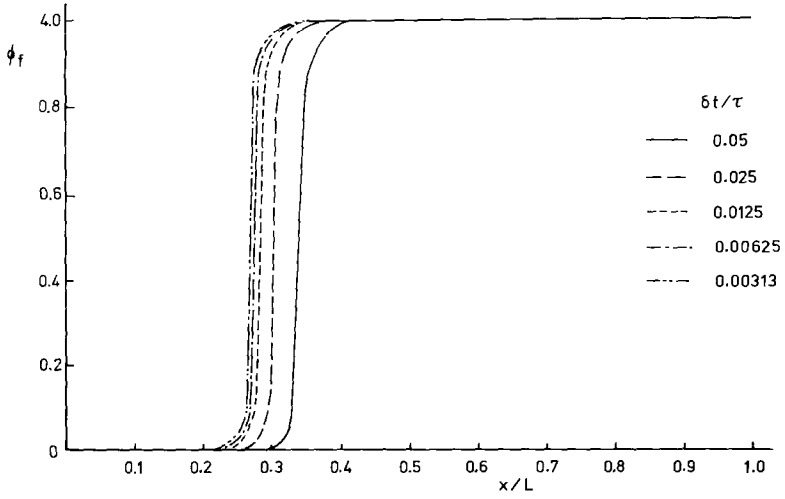

FIG. 4. Fuel concentration profiles at $t = 3\tau$ for chemical-kinetics controlled combustion.

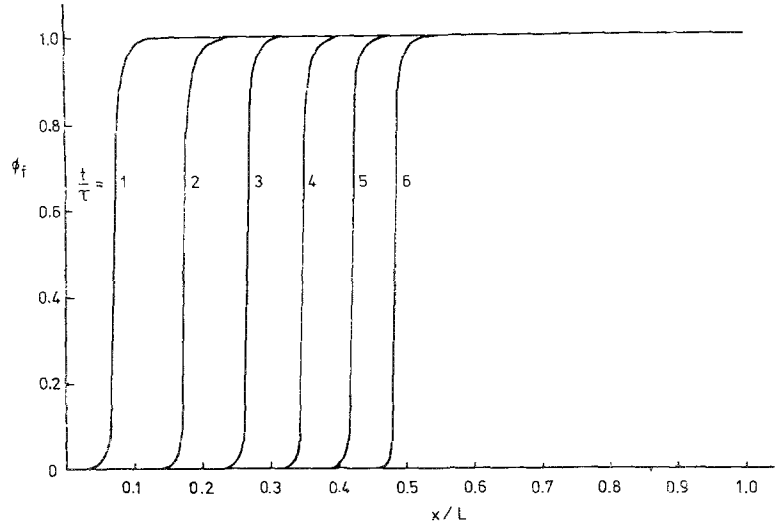

FIG. 5. Fuel concentration profiles at different times for chemical-kinetics controlled combustion.

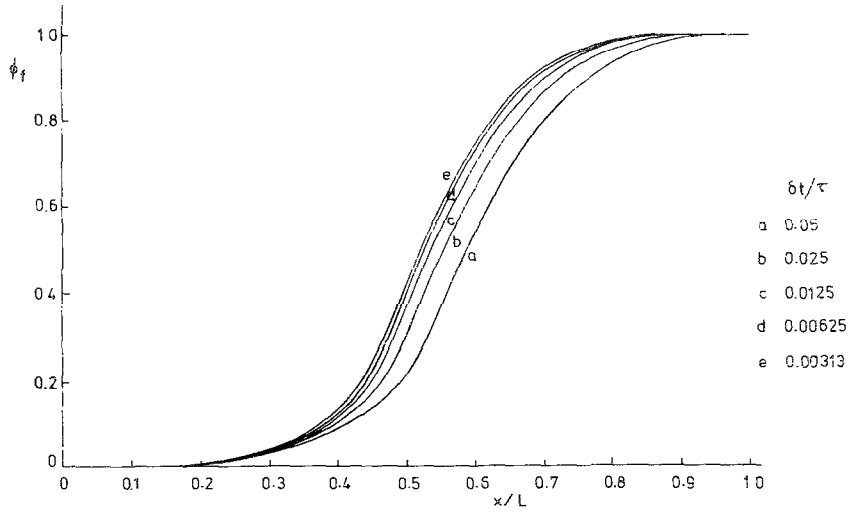

FIG. 6 Fuel concentration profile along one side of a two-dimensional chamber

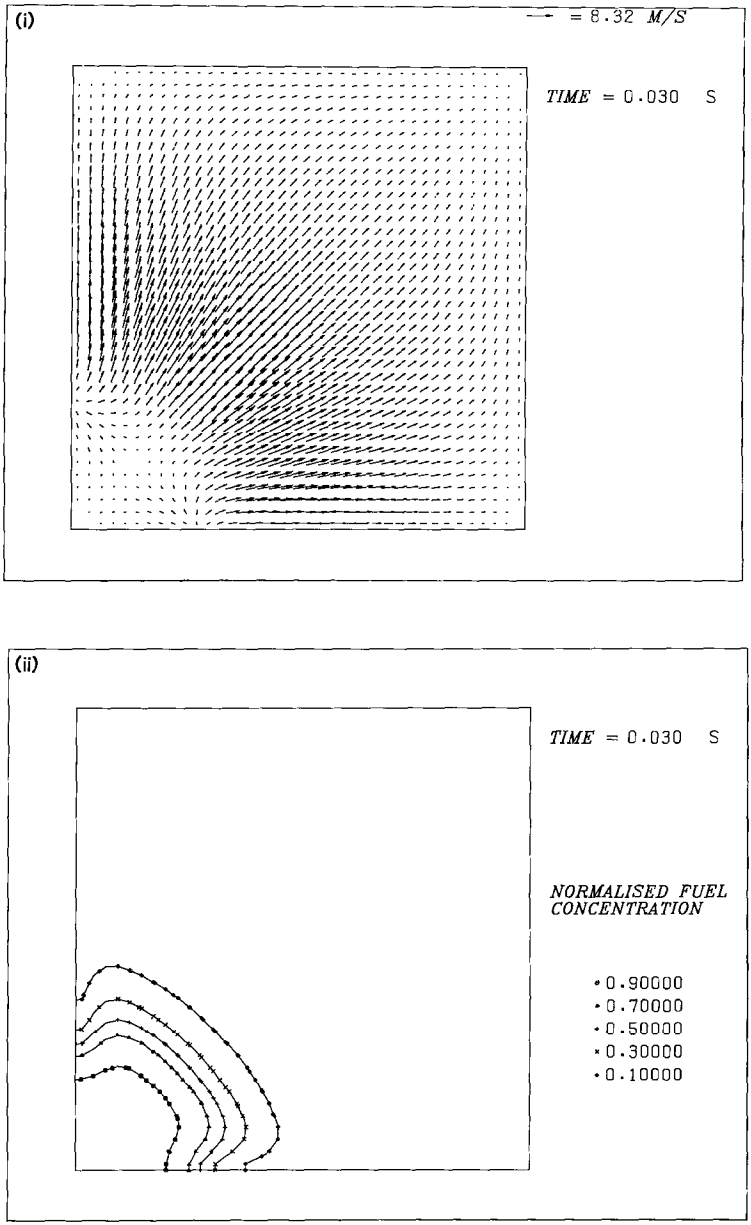

FIG. 7. Field variables in turbulence-controlled reaction in two-dimensional chamber at $t = 0.03$ s: (i) velocity vectors; (ii) fuel concentration; (iii) temperature.

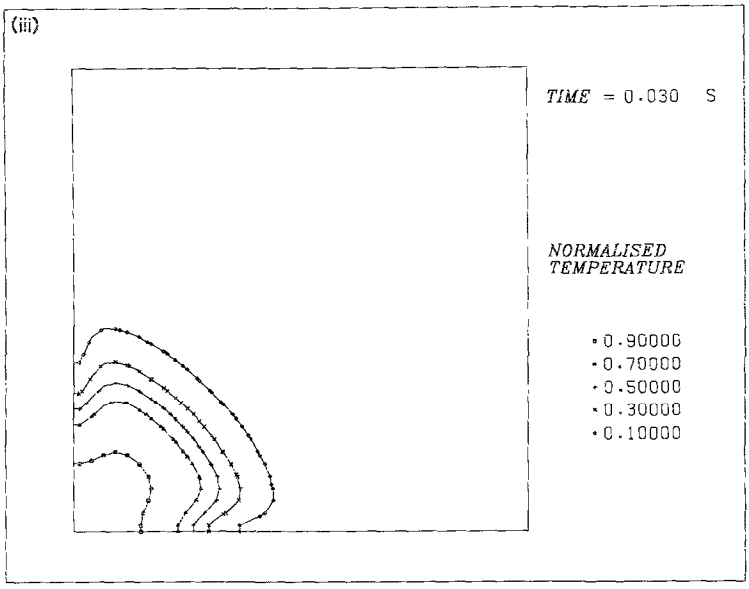

FIG. 7—*Continued*

jectured here that it is the temporal difference scheme, which is only first order accurate, that dictates such small δt. It should, of course, be remembered that the equations in this case are very "stiff" and very steep variations prevail, putting great demands on the scheme. The fuel concentration profiles, with the finest δt, at different time levels are shown in Fig. 5. Here a fine mesh of 400 cells is used to capture the sharpness of the flame front.

Two-Dimensional Reacting Flow

Here again two cases are presented; one with turbulent-mixing controlled reaction and the other with Arrhenius type of reaction. In the first case, a reacting flow with a constant effective viscosity (at a value typical of turbulent flow) is studied in a closed square chamber of 50×50 cm. The usual no-slip boundary conditions are imposed at the sides of the two-dimensional adiabatic chamber and a uniform grid of 40×40 cells was used. As was done in the previous case, burning was started

ber to be depleted at a rate which consumed $\frac{1}{16}$% of the total charge in the cell over a period of τ; after that, combustion is allowed to proceed at its own rate. For this case, calculations were performed for turbulent-mixing controlled combustion with the same values for coefficients A and B, mixing time scale, τ, and viscosity as those used in the one-dimensional case.

As in the one-dimensional case, computations were first performed with the iterative scheme using various values of δt to find the value δt_0 for which the temporal errors become negligible. The exercise was then repeated with the present

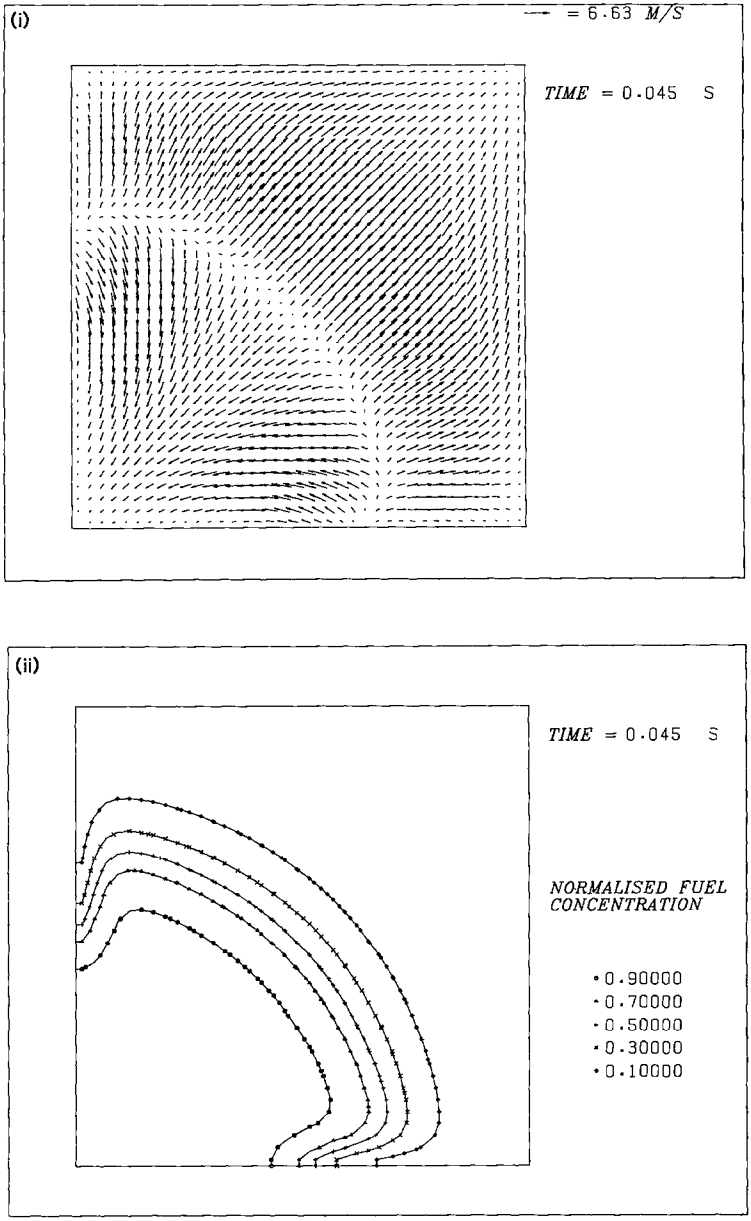

FIG. 8. Field variables in turbulence-controlled reaction in two-dimensional chamber at $t = 0.045$ s: (i) velocity vectors; (ii) fuel concentration; (iii) temperature.

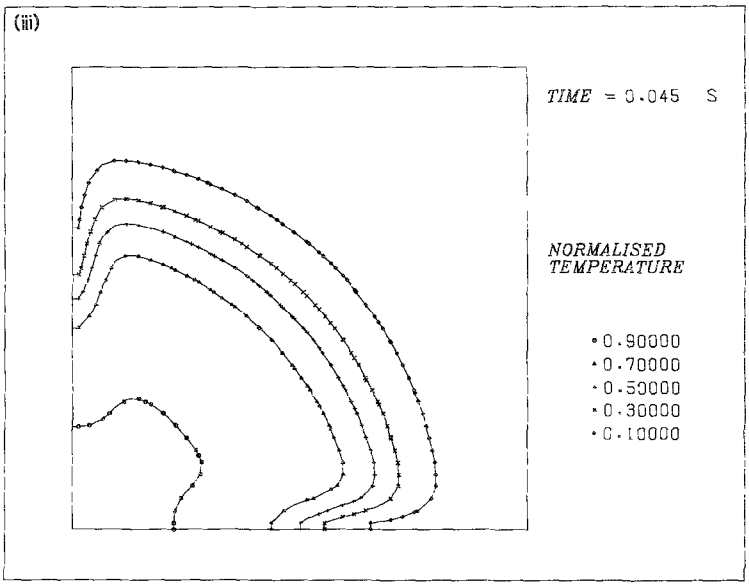

FIG. 8—*Continued*

method using time-steps which are multiples of δt_0. The results of these computations are displayed in Fig. 6 which shows the predicted reactedness at $t = 3\tau$ along one of the sides adjacent to the corner where ignition was initiated. Once again, it is clear that a time-step independent solution is obtained with PISO at the same step size as the iterative scheme, i.e., at $\delta t/\delta t_0 = 1$. The distributions of velocity, fuel concentration, and temperature (both normalised as before) at two time levels are

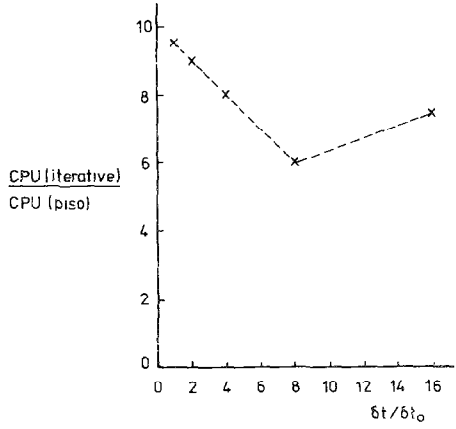

FIG. 9. Ratio of computing time of iterative/present method.

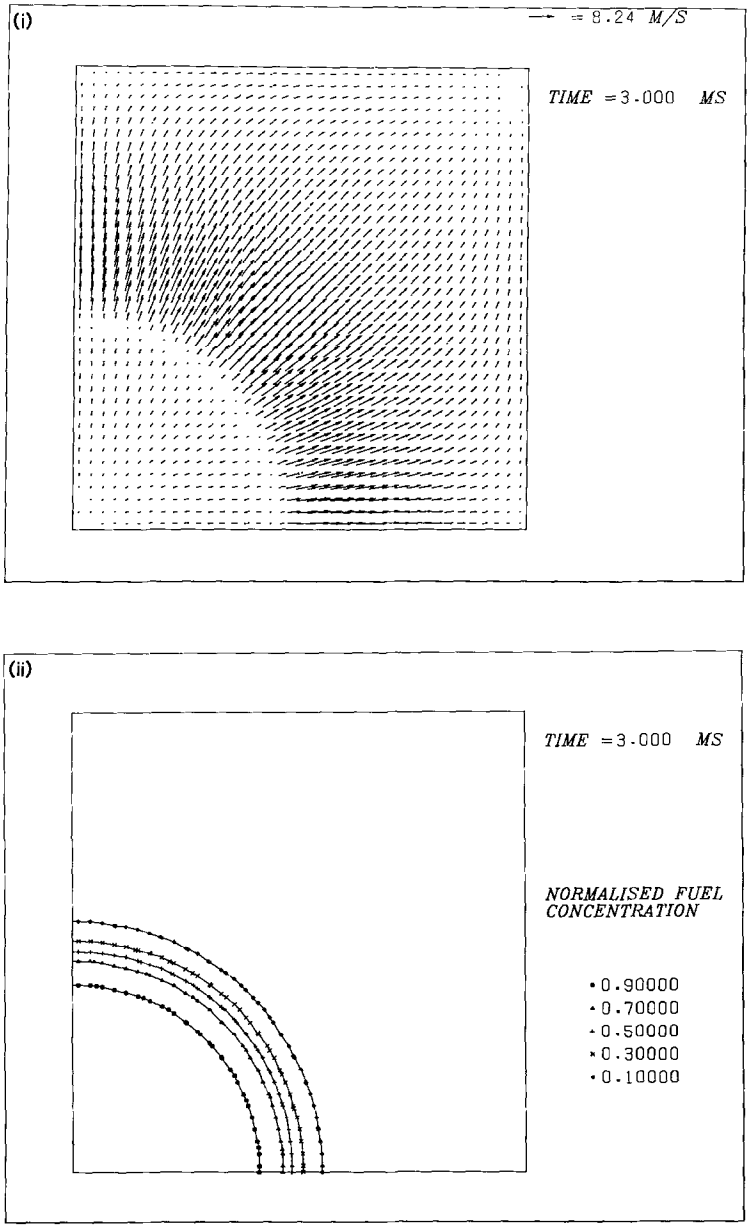

FIG. 10. Field variables in chemical-kinetics controlled reaction in two-dimensional chamber at $t = 3$ ms: (i) velocity vectors; (ii) fuel concentration; (iii) temperature.

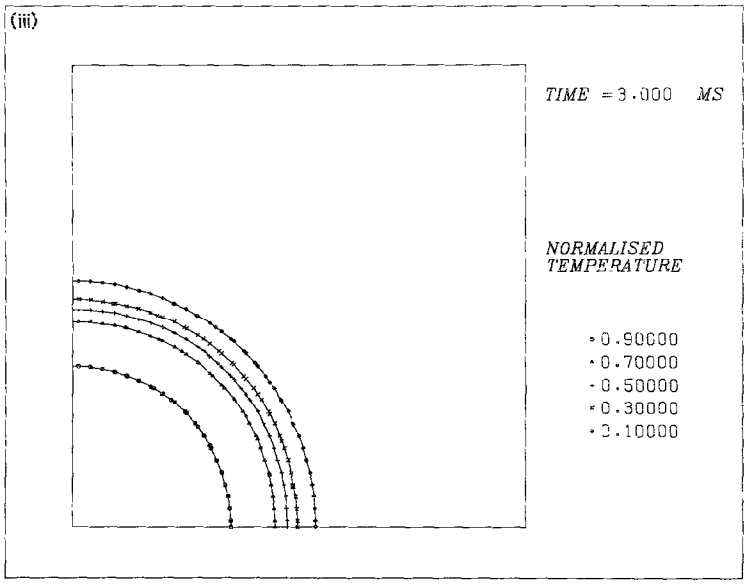

FIG. 10—*Continued*

illustrated in Figs. 7 to 8; the computation was performed with the finest time-step size. The results appear to be plausible.

In Fig. 9, the ratio of computing effort required by the iterative method to that by PISO is plotted as a function of the time-step size. It is evident that PISO is not only able to cope with large δt, but it is much faster, especially when a time-accurate solution ($\delta t/\delta t_0 = 1$) is required.

In the second case, the same 40×40 mesh was employed in a square chamber of 5×5 cm, the reduction in size from the previous case being necessitated by the desire to capture the thin flame by as many cells as possible without mesh refinement. Otherwise, the flame would have been far too thin to be captured by the mesh, and the calculations would have been somewhat meaningless. Other parameters are retained at their values presented for the previous cases. However, in order to investigate the flame propagation in the absence of wall effects, full slip was assumed at the walls; this should give a cylindrical flame front. Figs. 10 and 11 which display the velocity vector field and the normalised fuel concentration and temperature contours at two time levels, indeed show that the flame front is cylindrical. They also exhibit that a fairly thin flame front is predicted as is expected from a chemical-kinetics controlled reaction.

CONCLUSIONS

The PISO method of [1] is extended and suitably modified to handle the strong coupling arising in the equations governing reacting flows. This entails not only the

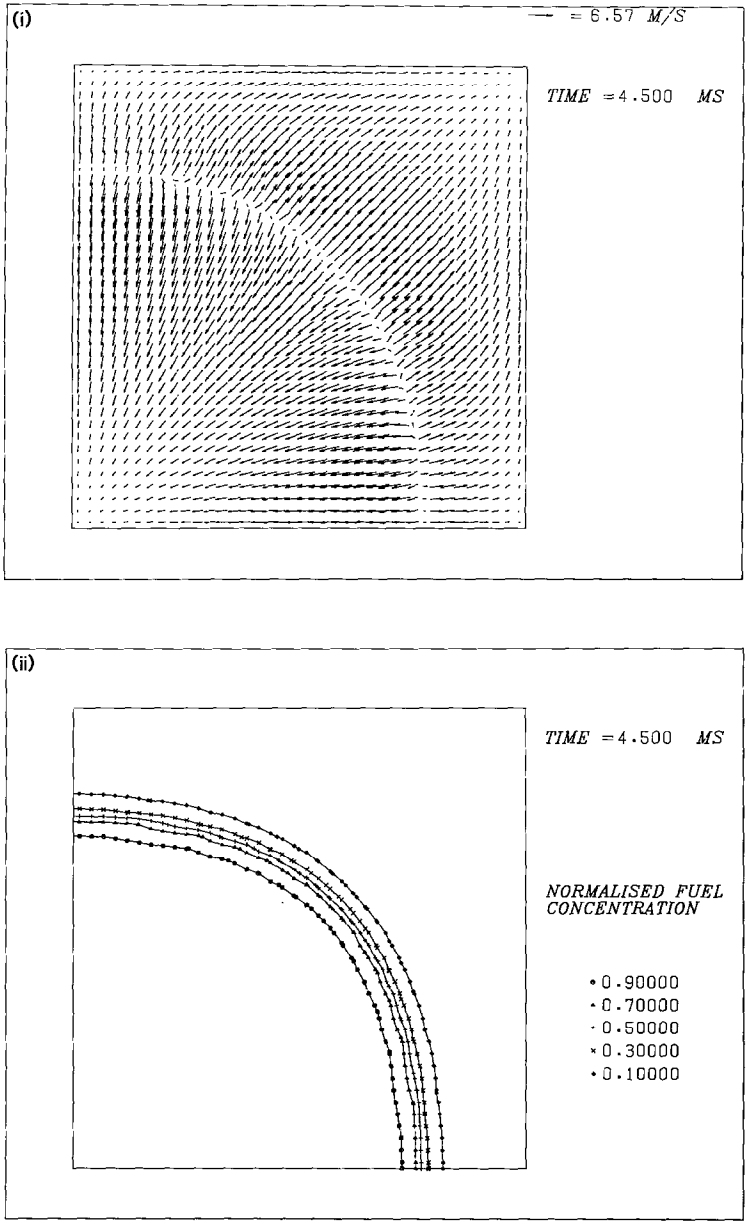

FIG. 11. Field variables in chemical-kinetics controlled reaction at $t = 4.5$ ms: (i) velocity vectors; (ii) fuel concetration; (iii) temperature.

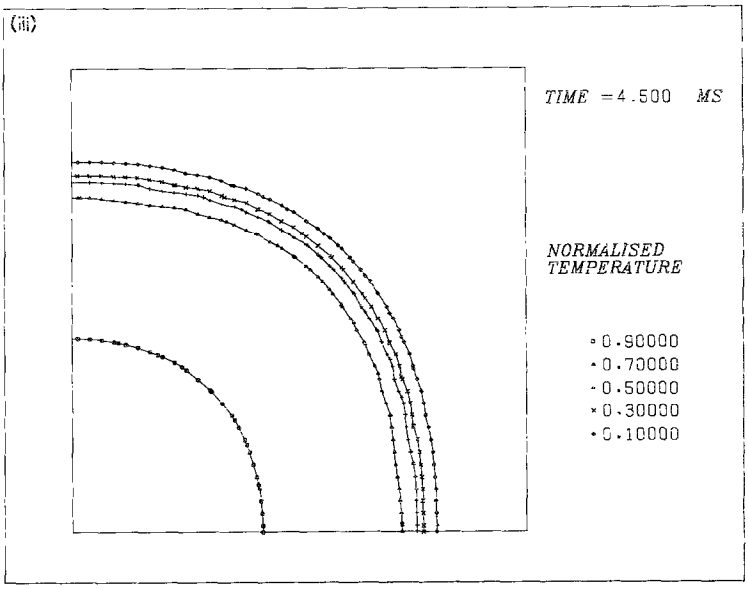

FIG. 11—*Continued*

handling of additional source terms, but also the accounting for the rapid variations in convective coefficients due to steep density changes. Reorganisation of the splitting sequence has been necessary to achieve all this.

The new scheme was applied to two problems of unsteady reacting flows, in one- and two-dimensional closed chambers. The results demonstrate that the splitting process undermines neither temporal accuracy nor stability. Comparison with an existing iterative scheme reveals that reacting flow PISO is several times faster than its iterative counterpart, and that the scheme is equally capable of handling turbulent-mixing and chemical-kinetics controlled combustion.

ACKNOWLEDGMENT

The authors wish to thank Dr. A. Folefac of the Department of Mineral Resources Engineering for

REFERENCES

1. R. I. ISSA, *J. Comput. Phys.* **62**, 40 (1986).
2. R. I. ISSA, A. D. GOSMAN, AND A. P. WATKINS, *J. Comput. Phys.* **62**, 66 (1986).
3. F. C. LOOCKWOOD, S. M. A. RIZVY, G. K. LEE, AND H. WHALEY, "Proceedings 20th Int. Combustion Symp., 1984," p. 513.

4. D. S. JANG, R. JETLI, AND S. ACHARYA, *Numer. Heat Transfer* **10**, 209 (1986).
5. R. J. KEE AND J. A. MILLER, *AIAA J.* **16**, 169 (1978).
6. J. B. GREENBERG, *Int. J. Num. Methods Fluids* **4**, 653 (1984).
7. B. F. MAGNUSSEN AND B. H. HJERTAGER, in *Proceedings 16th Symposium (Int) on Combustion* (Combustion Institute, New York, 1976), p. 719.
8. L. S. CARETTO, A. D. GOSMAN, S. V. PATANKAR, AND D. B. SPALDING, in *Proceedings, 3rd Int. Conf. on Numerical Methods in Fluid Dynamics*, 1972, p. 60.
9. S. V. PATANKAR, *Numerical Heat Transfer and Fluid Flow*. (McGraw–Hill, New York, 1980).
10. J. P. VAN DOORMAAL AND G. D. RAITHBY, *Numer. Heat Transfer* **7**, 147 (1984).
11. B. AHMADI-BEFRUI, A. D. GOSMAN, F. C. LOCKWOOD, AND A. P. WATKINS, *Trans. SAE* 636 (1981).